

maximum energy underestimated the effect of secondary particles produced in the attenuators.

The absolute value of the $C^{12}(p,pn)C^{11}$ cross section at 350 Mev is significantly lower than that reported earlier,¹ and the difference is believed to be due to the increased accuracy of absolute β counting that has been achieved in the last few years. Readjustment of the excitation function on the basis of our results leads to improved agreement between the p - p scattering cross sections measured at Berkeley and those measured elsewhere⁸ using the $C^{12}(p,pn)C^{11}$ reaction to monitor the proton beam. The reported results of other experiments will be affected by the readjustment of the

excitation function; a partial list of such experiments is given in references 6 to 8.

ACKNOWLEDGMENTS

The authors are happy to acknowledge the support and assistance of Dr. C. M. VanAtta. We also wish to thank Frank L. Adelman, John Ise, Jr., Larry Schechter, Marian N. Whitehead, Donald A. Hicks, and Robert M. Main for assistance in collecting data, and the cyclotron crew under the direction of James Vale for helpful cooperation. Joe Murray and Nahmin Horwitz assisted in the β - γ coincidence measurements.

PHYSICAL REVIEW

VOLUME 101, NUMBER 1

JANUARY 1, 1956

Production of Deuterons in High-Energy Nucleon Bombardment of Nuclei and Its Bearing on Nuclear Charge Distribution

WILMOT N. HESS AND BURTON J. MOYER

Radiation Laboratory, University of California, Berkeley, California

(Received August 2, 1955)

A study has been made of deuterons produced at wide angles to a beam of 300-Mev neutrons and a beam of 300-Mev protons. The cross-section dependence on atomic number for these deuterons for light elements can be written as $\sigma = kA^{1.2}$. This fact and the energy spectra and angular distribution of the deuterons show that the process that forms these deuterons is related to the indirect pick-up process described by Bransden. This is a two-step process in which the incident nucleon, or its collision partner, is scattered and then picks up a deuteron-forming partner in the same nucleus. A yield of tritons has also been observed which has the same A -dependence and is presumably made by a similar process. The A -dependence of the deuteron-production cross section also suggests that these deuterons are made on the nuclear surface. Because of this A dependence, a comparison of the deuteron yields using an incident neutron beam and an incident proton beam can give information about the relative numbers of neutrons and protons on the surface of the nucleus. An analysis of this sort leads to a possible conclusion that for heavy nuclei there is a nuclear skin rich in neutrons. For light nuclei the effect is not observed. If this skin is composed only of neutrons its thickness must be about 0.8×10^{-13} cm for lead.

I. INTRODUCTION

AMONG the various phenomena that reveal the constitution and organization of the nucleus are the identity and characteristics of the secondary particles that emerge under controlled bombarding conditions. The deuteron as a secondary particle has been of considerable interest, since its small binding energy invites questions as to the processes by which it may emerge intact, particularly in high-energy events. The elucidation of these phenomena has contributed to the "pick-up" concepts which have been prominent in recent nuclear reaction theory.

In 1952, at this laboratory, Clark¹ observed a yield of deuterons at 40° to a 340-Mev proton beam from a carbon target. Because these deuterons were made at a large angle to a high-energy beam, it was improbable that they were direct pick-up deuterons.^{2,3} Because of

the way they are formed, direct pick-up deuterons are quite sharply peaked along the direction of the beam, and have energies fairly closely related to the beam energy. It is expected that there will be considerably fewer direct pickup deuterons at 340 Mev than at 100 Mev. At about the time Clark first observed these deuterons, Bransden⁴ wrote a theoretical paper describing a method for producing deuterons of characteristics similar to those observed. Quoting from Bransden's paper, "Deuterons may be formed as the result of a second-order process in which a nucleon of relatively small momentum (produced by the collision of the incident neutron with a nucleon in the target nucleus) picks up a second nucleon in the target nucleus to form a deuteron."

This mechanism of formation could account for the observed deuterons. It is known that the energy spectrum of protons quasi-elastically scattered from carbon at 40° from a 340-Mev proton beam shows a character-

¹ D. D. Clark (private communication).

² J. Hadley and H. York, *Phys. Rev.* **80**, 345 (1950).

³ G. F. Chew and M. L. Goldberger, *Phys. Rev.* **77**, 470 (1950).

⁴ B. H. Bransden, *Proc. Phys. Soc. (London)* **A65**, 738 (1952); and private communication.

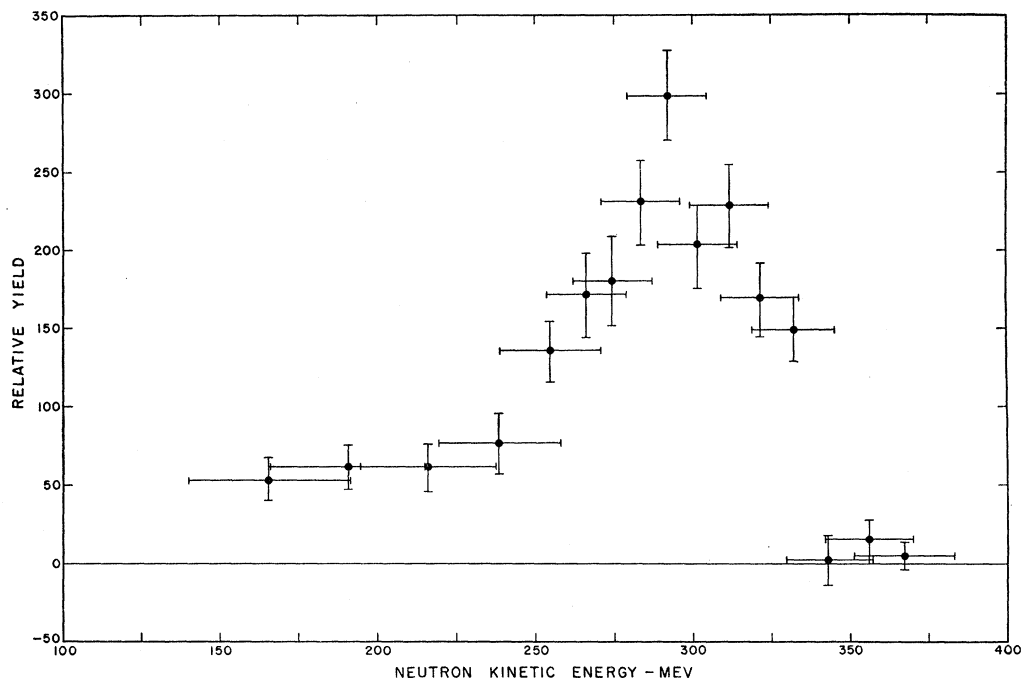


FIG. 1. Neutron energy spectrum produced from 340-Mev protons bombarding 2 inches of Be.

istic range of energies below the bombarding energy,⁵ and some of the scattered protons can pick up partners having suitable momenta to make deuterons. The pickup process would form deuterons traveling roughly in the direction of the scattered protons. In this way we can obtain a considerable yield of deuterons, at larger angles from the beam than the direct pick-up process would allow. Such deuterons would be similar to those Clark observed.

II. EXPERIMENTAL APPARATUS AND PROCEDURE

A. Cyclotron Beams

This experiment was performed with the external high-energy proton and neutron beams of the 184-inch Berkeley synchrocyclotron. The neutron beam was produced by bombarding a 2-inch-thick Be target with 340-Mev protons. The neutron spectrum⁶ obtained in this way is shown in Fig. 1, in which the peak of the spectrum is seen to be at about 300 Mev.

A copper energy degrader placed in the deflected beam reduced the energy of the proton beam from 340 Mev to 300 Mev to allow direct comparison with the neutron-beam experiments.

The scattering targets used were lithium, carbon, aluminum, copper, cadmium, lead, uranium, and polyethylene, $(\text{CH}_2)_n$.

⁵ Cladis, Hess, and Moyer, *Phys. Rev.* **87**, 425 (1952).

⁶ This was obtained by Ball, Cladis, and Hess by the method given by Cladis, Hadley, and Hess, *Phys. Rev.* **86**, 110 (1952).

B. Particle Identification by Measurement of E and dE/dx

1. General Experimental Method

A large part of the information in this experiment was obtained by a particle-detection method which measured dE/dx and E for the scattered charged particles. This is accomplished by using a telescope of three crystal scintillators, the crystal towards the target moderately thin and the second crystal thick enough to stop most of the scattered particles. The third crystal is used to detect the passage of particles too energetic to be stopped in the second crystal, which it was desirable to keep to a limited size. The apparatus is shown in Fig. 2. The particle energy loss in the thin crystal is related to dE/dx , and the energy loss in the second crystal to E of the incident particle. The measurement of these two parameters determines the mass and energy of the observed scattered particles (particles assumed to have one electronic charge). The relationship between E and dE/dx for various particles is plotted in Fig. 3.

2. Counters

The scintillators used in this experiment were made of terphenyl-impregnated polystyrene, and were viewed by RCA 5819 photomultipliers. The first and second scintillators—which measure, respectively, dE/dx and E of the incident particles—were also viewed by a pair of 1P21 photomultipliers on each scintillator in order to define a coincidence that could be used as an oscilloscope sweep trigger. Because of the thickness of the dE/dx crystal, the particles that passed through the

telescope had the following low-energy cutoffs:

- protons, $E > 36$ Mev;
- deuterons, $E > 48$ Mev;
- tritons, $E > 58$ Mev.

He³ and heavier particles were not observed in any measurable quantity, probably because the energy cutoff is too high. The energy cutoff for He³ is 125 Mev.

3. Electronics

Figure 2 shows the electronics used with the $E-dE/dx$ equipment. The pulses from the 5819 photomultipliers viewing the scintillators were exhibited on a model 517 Tektronix oscilloscope. The 1P21 signals were added, clipped, amplified, and fed into a double-coincidence circuit, the output of which was used to trigger the scope and was also recorded on a scaler. The scope face was photographed by a 35-mm free-running movie camera.

4. Calibration

Part of one run was devoted to calibrating the $E-dE/dx$ equipment. This was done by placing the scintillators directly in a low-intensity beam of monoenergetic particles. Deuterons were accelerated to 190 Mev in the cyclotron and then the energy of the deuterons was reduced by placing copper energy degraders in the deflected beam to obtain deuterons of 120 Mev

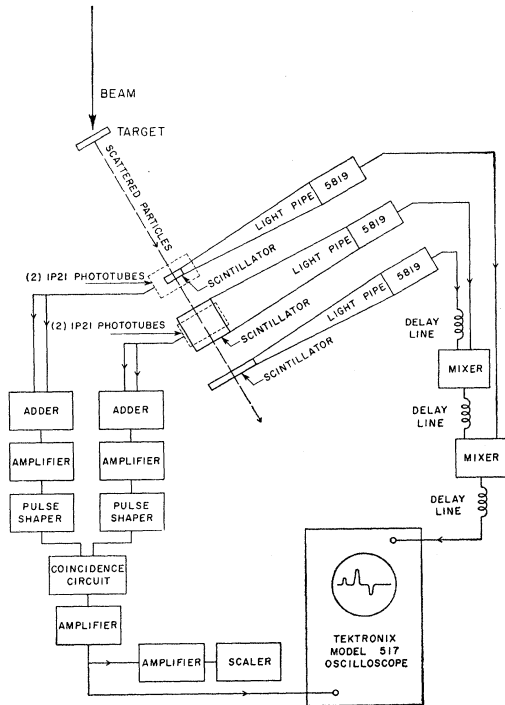


FIG. 2. Experimental apparatus used in the $E-dE/dx$ method.

and 50 Mev. Similarly, the 340-Mev proton beam was reduced to 110 Mev and to 40 Mev, and the pulse-height distribution produced in the counters was measured for these various incident particles. The results of these measurements are shown in Fig. 4, though only the central part of the 40-Mev proton beam pulse-height distribution is shown because straggling in the extensive energy degradation made this distribution so wide. The curves drawn on Fig. 4 are the E vs dE/dx relationship plotted on Fig. 3, and the theoretical curves have been fitted to the calibration data at the 110-Mev proton point. It is seen that the theoretical curve fits the experimental data satisfactorily.

C. $H\rho$ -Range Method

Part of the data taken using the 300-Mev proton beam were obtained by using $H\rho$ and range to determine mass and energy of the scattered particle. This was done by bending the paths of the scattered particles through a magnetic field and then counting the numbers of particles appearing at various exit positions by a 35-channel set of scintillation counters. This equipment is quite similar to that used by Cladis.⁵ The separation of deuterons from protons was accomplished by placing graded, tapered absorbers in front of the 35-channel counters. Figure 5 shows the experimental arrangement. The absorbers were made to be a certain fraction of a deuteron range thick at each point. Several of these wedge-shaped absorbers were provided, having thicknesses of $0.3R_D$, $0.6R_D$, $1.2R_D$, and $2.0R_D$.

The total counting rate of the 35-channel counters were determined as a function of absorber thickness, and a curve of this sort for aluminum is shown in Fig. 6.

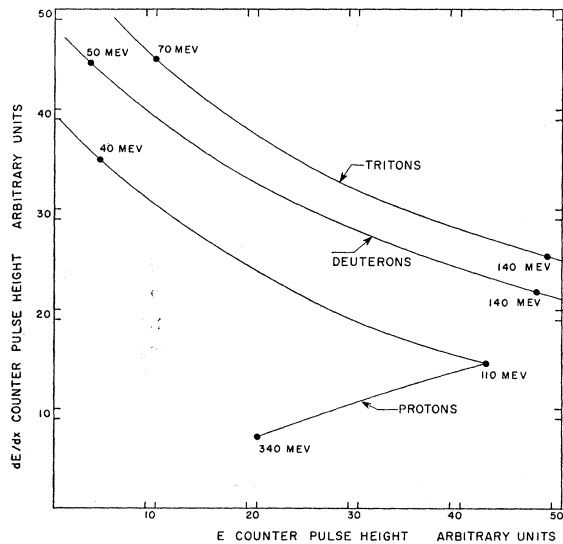


FIG. 3. The $E-dE/dx$ relationship for various particles.

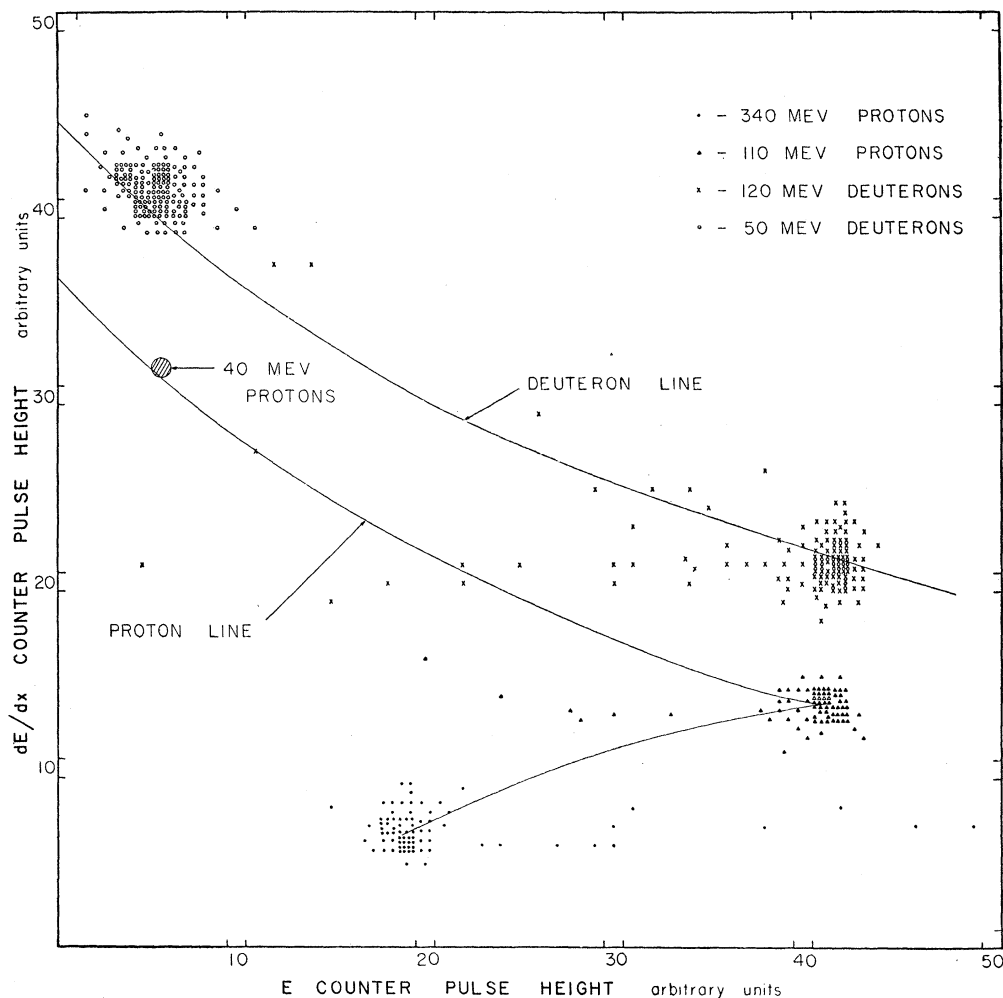


FIG. 4. $E-dE/dx$ calibration data taken with various monoenergetic beams.

The dip at the deuteron range is quite apparent, indicating the fraction of deuterons.

III. ANALYSIS OF DATA

A sample of the $E-dE/dx$ data taken with an Al target at 40° is shown on Fig. 7. These data show clearly the proton line and also the deuteron line. Also less evident, but present, is a contribution of tritons. If the proton, deuteron and triton lines are drawn in on this plot as in Fig. 4, and lines of constant mass are then drawn between these three lines, a particle-mass distribution curve can be obtained by counting the events lying between the various lines. A mass spectrum arrived at in this way is shown in Fig. 8. It is seen that the deuteron peak is quite well separated from the proton distribution, and also that there are some tritons present and that they are moderately well separated from the deuterons.

The counting rate of the scaler that was recording the number of scope traces was used to obtain the differential cross section for all scattered charged particles

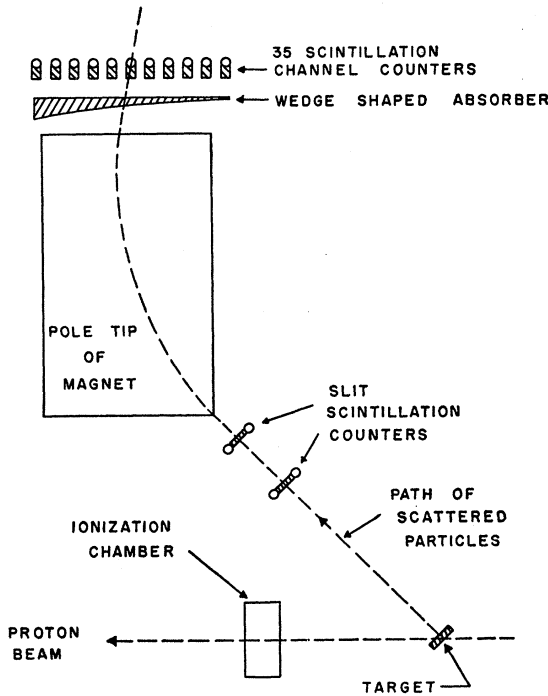
from a given target, which is expressed by

$$\sigma(\theta) = \frac{C(\theta)}{Nn} \left(\frac{1}{\Omega\epsilon} \right),$$

where we have $C(\theta)$ = scaler counts at angle θ , N = corresponding beam flux, n = target atoms/cm², Ω = solid angle, and ϵ = counting efficiency.

The neutron beam flux was measured by employing CH₂-C target differences together with known $n-p$ cross sections. Proton beam flux was determined by a calibrated ionization chamber which the beam traversed.

The cross sections $\sigma(\theta)$ result from a combination of protons, deuterons, and tritons, and in order to get individual particle cross sections we return to the pulse-height data. By superimposing proton-deuteron and deuteron-triton separation lines, which can be obtained from Fig. 3, onto the pulse-height data as shown in Fig. 7, we can determine the fractions of the total counts that are protons, deuterons, and tritons. The target-out yield must be subtracted away in order to


 FIG. 5. Experimental apparatus used in the $H\rho$ -range method.

get these fractions. Using these numbers, we can get the cross sections for production of protons, deuterons, and tritons at angle θ from nucleons bombarding element X :

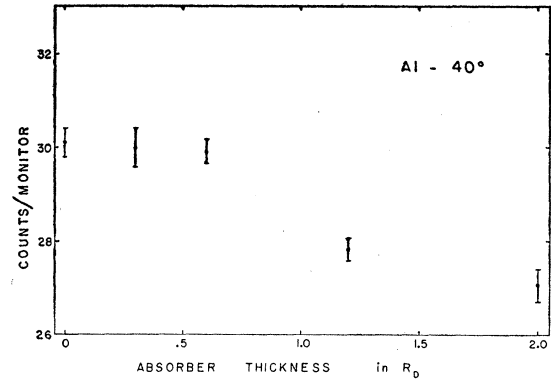
$$\sigma_{(\text{nucleon} + X \rightarrow p)}(\theta) = \sigma(\theta) \left[\frac{\text{protons}}{\text{all particles}} \right];$$

$$\sigma_{(\text{nucleon} + X \rightarrow d)}(\theta) = \sigma(\theta) \left[\frac{\text{deuterons}}{\text{all particles}} \right];$$

$$\sigma_{(\text{nucleon} + X \rightarrow t)}(\theta) = \sigma(\theta) \left[\frac{\text{tritons}}{\text{all particles}} \right].$$

Tables I and II give a summary of the cross sections obtained in this way. The deuteron differential cross sections for proton bombardment of various elements at an angle of 40° to the beam are shown in Fig. 9. All the differential proton cross sections measured in the course of the experiment are plotted against A in Fig. 10.

We can also obtain energy spectra from the pulse-height data as shown in Fig. 7. Taking the results of the calibration run as shown in Fig. 4, and using the calculated E vs dE/dx lines as shown in Fig. 3, we can draw lines of known energy intersecting the E vs dE/dx lines. By counting the numbers of events between two such lines and dividing by the energy interval, we obtain the energy spectra. Proton spectra obtained from the E vs dE/dx data are shown in Figs. 11, 12, and 13.


 FIG. 6. An absorber curve obtained using the $H\rho$ -range method.

Deuteron energy spectra made by E vs dE/dx and $H\rho$ -range methods for an angle of 40° are shown in Fig. 14.

The absorber curves, such as shown in Fig. 6, obtained by use of the magnet, can be analyzed to get the differential cross sections for production of deuterons. The magnitude of this dip at $R_D=1$ compared to the height of the curve for an absorber thickness of $R_D=0$ gives the fraction of charged particles that are deuterons. Correction must be made for proton nuclear absorption in the tapered absorbers.

IV. CALCULATION OF DEUTERON YIELDS AND ENERGY SPECTRA

Employing the indirect pickup-process model proposed for the deuteron-formation mechanism, and starting with known spectra and yields of scattered protons, we may try to fit the deuteron spectra and yields. We write, for the carbon nucleus as an example, that the cross section for producing indirect pick-up deuterons, using an incident proton beam, is the product of the cross section for quasi-elastic scattering of the beam protons and the probability that a scattered nucleon picks up a partner to form a deuteron. Thus

$$\frac{d\sigma(p+C \rightarrow d)}{d\Omega dE} = \frac{d\sigma(p+C \rightarrow p)}{d\Omega dE} (P_1) + \frac{d\sigma(p+C \rightarrow n)}{d\Omega dE} (P_2).$$

The first term on the right above is the contribution from scattered protons picking up neutrons, and the second term is due to scattered neutrons picking up protons. P_1 is the probability for a scattered proton to pick up a neutron to form a deuteron and P_2 is the probability for a scattered neutron to pick up a proton.

In the case of the proton beam we have measured

$$\frac{d\sigma(p+C \rightarrow p)}{d\Omega dE} \text{ and } \frac{d\sigma(p+C \rightarrow d)}{d\Omega dE}, \text{ but not } \frac{d\sigma(p+C \rightarrow n)}{d\Omega dE}.$$

For the shape of the quasi-elastic scattered-neutron energy spectrum, the last term above, we take the

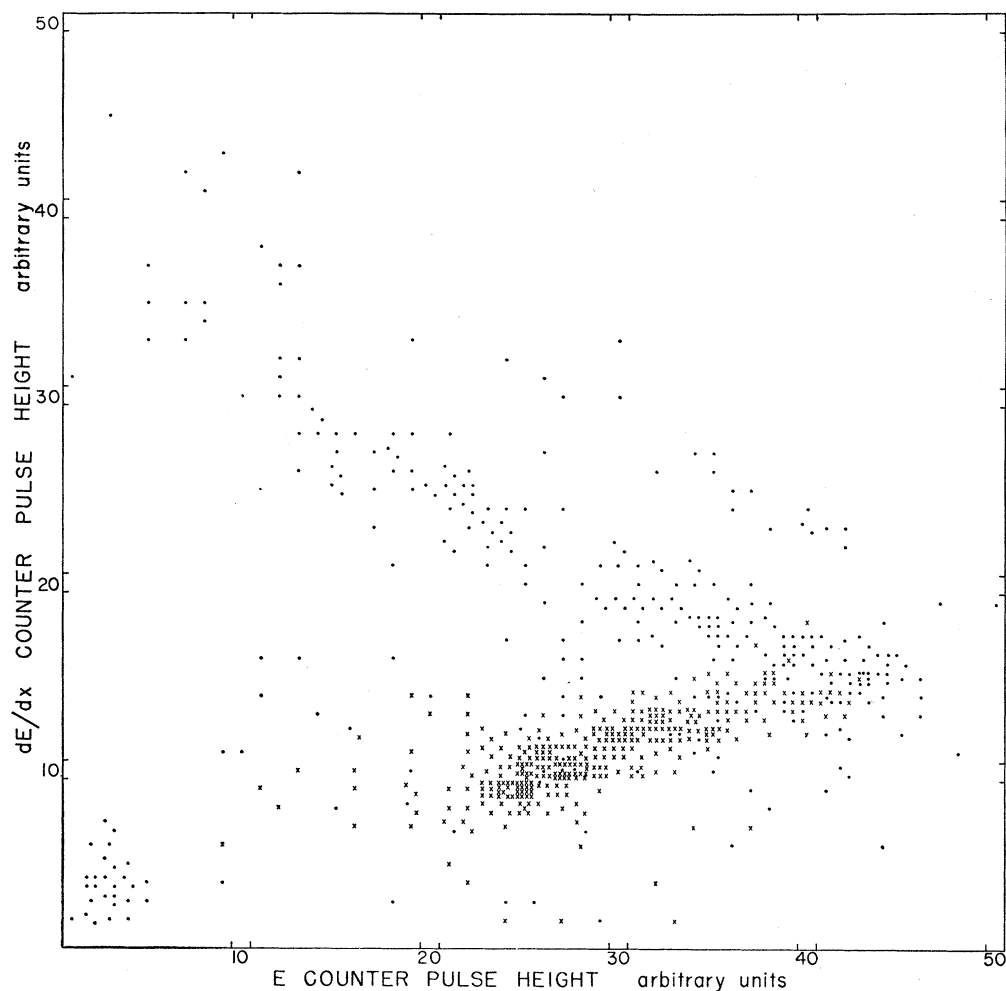


FIG. 7. A sample of data taken using the $E-dE/dx$ method.

measured proton spectrum and change it point by point by the ratio of the free-nucleon differential cross sections, $\sigma_{np}(\theta)/\sigma_{pp}(\theta)$. The areas underneath the spectra were normalized to the measured differential cross

sections $\sigma(p+C \rightarrow p)$ and $\sigma(n+C \rightarrow p)$, since the latter should be expected to be equivalent to $\sigma(p+C \rightarrow n)$. The probability that a proton picks up a neutron P_1 should equal the probability that a neutron picks up a

TABLE I. Differential cross sections obtained using 300-Mev protons. (All values are in millibarns/steradian.)

	Lithium	Carbon	Aluminum	Copper
$\sigma_{p+X \rightarrow p}(26^\circ)$...	70.0 \pm 4.0	130.1 \pm 5.0	188.5 \pm 7.0
$\sigma_{p+X \rightarrow p}(40^\circ)$	35.3 \pm 3.0	52.3 \pm 4.0	89.0 \pm 4.0	142.8 \pm 6.0
$\sigma_{p+X \rightarrow d}(26^\circ)$...	1.72 \pm 0.41	3.54 \pm 0.75	6.44 \pm 1.32
$\sigma_{p+X \rightarrow d}(40^\circ)$	1.16 \pm 0.31	1.90 \pm 0.35	4.69 \pm 0.48	7.86 \pm 1.04
$\sigma_{p+X \rightarrow d}(60^\circ)$...	1.42 \pm 0.30
$\sigma_{p+X \rightarrow t}(26^\circ)$...	0.120 \pm 0.068	0.150 \pm 0.108	0.316 \pm 0.179
$\sigma_{p+X \rightarrow t}(40^\circ)$	0.079 \pm 0.042	0.148 \pm 0.069	0.415 \pm 0.108	0.260 \pm 0.189
$\sigma_{p+X \rightarrow t}(60^\circ)$...	0.024 \pm 0.041
	Cadmium	Lead	Uranium	
$\sigma_{p+X \rightarrow p}(26^\circ)$...	290.0 \pm 12.0
$\sigma_{p+X \rightarrow p}(40^\circ)$	193.2 \pm 9.0	234.0 \pm 12.0	251.0 \pm 11.0	...
$\sigma_{p+X \rightarrow d}(26^\circ)$...	13.9 \pm 2.86
$\sigma_{p+X \rightarrow d}(40^\circ)$	11.22 \pm 1.20	18.0 \pm 2.14	16.80 \pm 1.68	...
$\sigma_{p+X \rightarrow d}(60^\circ)$
$\sigma_{p+X \rightarrow t}(26^\circ)$...	1.22 \pm 0.550
$\sigma_{p+X \rightarrow t}(40^\circ)$	0.492 \pm 0.296	2.035 \pm 0.596	0.191 \pm 0.248	...
$\sigma_{p+X \rightarrow t}(60^\circ)$

TABLE II. Differential cross sections obtained using 300-Mev neutrons. (All values are in millibarns/steradian.)

	Lithium	Carbon	Aluminum	Copper
$\sigma_{n+X \rightarrow p}(26^\circ)$...	27.7 ± 2.0	49.2 ± 3.0	76.3 ± 5.0
$\sigma_{n+X \rightarrow p}(40^\circ)$	9.6 ± 0.85	16.15 ± 0.77	29.7 ± 1.4	46.8 ± 1.9
$\sigma_{n+X \rightarrow d}(26^\circ)$...	2.80 ± 0.40	4.15 ± 0.50	7.08 ± 0.86
$\sigma_{n+X \rightarrow d}(40^\circ)$	1.13 ± 0.17	2.09 ± 0.20	3.87 ± 0.40	5.31 ± 0.62
$\sigma_{n+X \rightarrow t}(26^\circ)$...	0.311 ± 0.133	0.860 ± 0.195	0.715 ± 0.295
$\sigma_{n+X \rightarrow t}(40^\circ)$	0.092 ± 0.026	0.291 ± 0.061	0.599 ± 0.124	0.992 ± 0.196
	Cadmium	Lead	Uranium	
$\sigma_{n+X \rightarrow p}(26^\circ)$...	120.2 ± 9.0	...	
$\sigma_{n+X \rightarrow p}(40^\circ)$	64.2 ± 2.4	80.4 ± 3.3	83.3 ± 3.3	
$\sigma_{n+X \rightarrow d}(26^\circ)$...	9.71 ± 1.60	...	
$\sigma_{n+X \rightarrow d}(40^\circ)$	8.85 ± 0.78	10.03 ± 1.12	9.97 ± 1.17	
$\sigma_{n+X \rightarrow t}(26^\circ)$...	1.60 ± 0.61	...	
$\sigma_{n+X \rightarrow t}(40^\circ)$	0.820 ± 0.217	1.948 ± 0.395	1.518 ± 0.380	

proton P_2 for carbon, since the matrix element entering into both probabilities should be the same, and the number of neutrons is the same as the number of protons, and there is not expected to be any effective difference in the distribution of neutrons and protons for the carbon nucleus.

Using this information, and assuming that the energy dependence of the pick-up probability can be written as a power law in the kinetic energy of the scattered nucleon, we take

$$P_1 = P_2 = kE^{-n}_{\text{scattered nucleon}},$$

where E is the energy of the beam nucleon after it has been scattered but before it picks up a second nucleon in the target nucleus to form a deuteron. Substituting this into the equation above and arbitrarily choosing a particular value for n , we get the deuteron energy

spectrum. The pick-up deuteron energy is related to, but not the same as, the scattered-nucleon energy. In a $p-d$ collision leading to the formation of a direct pick-up deuteron the energy relation is

$$E_{\text{pick-up deuteron}} = (8/9)E_{\text{proton}} \cos^2 \phi,$$

where ϕ is the angle between the direction of motion of the incident proton and the pick-up deuteron formed in the event. We may write as an approximation for the energy relation in a complex nucleus,

$$E_{\text{pick-up deuteron}} = (8/9)E_{\text{scattered nucleon}} \cos^2 \theta - B,$$

where $E_{\text{scattered nucleon}}$ is the energy of the beam nucleon after it has scattered, but before it picks up to form a deuteron; θ is the angle between the directions of motion of the scattered nucleon and the pick-up deuteron; and B is similar to the binding energy of the nucleon which is removed from the target nucleus in forming the pick-up deuteron. The value of B can be evaluated from the data of Hadley and York.² Chew and Goldberger³

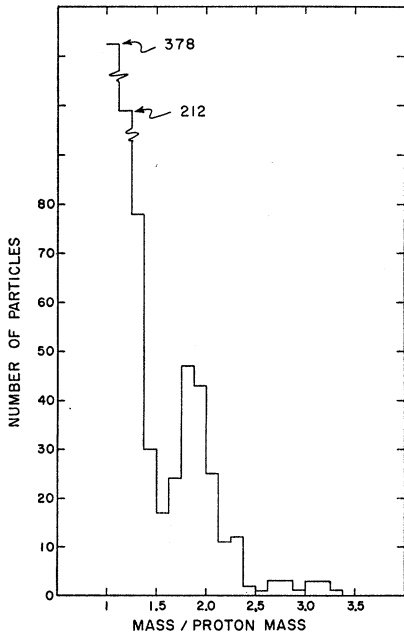


FIG. 8. Mass spectrum obtained from $E-dE/dx$ data.

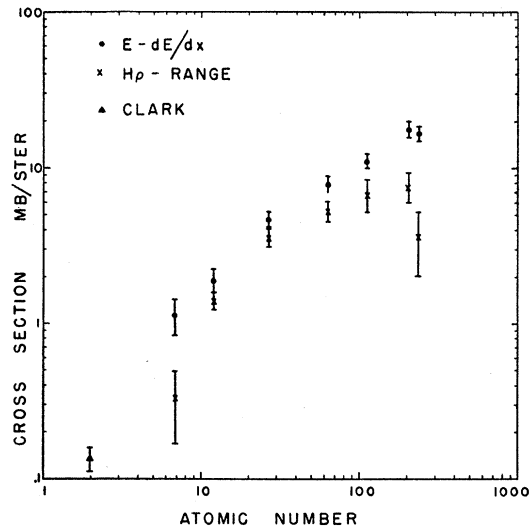


FIG. 9. Deuteron differential cross sections at 40° .

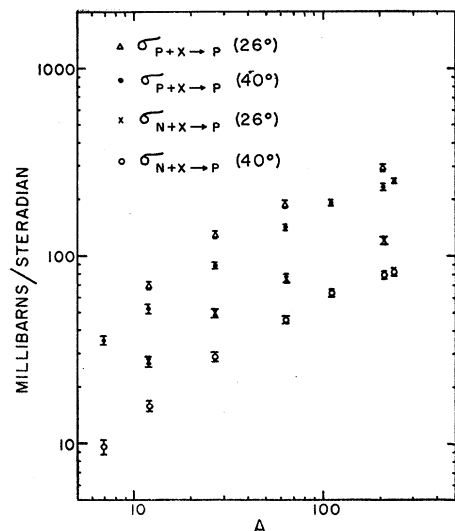


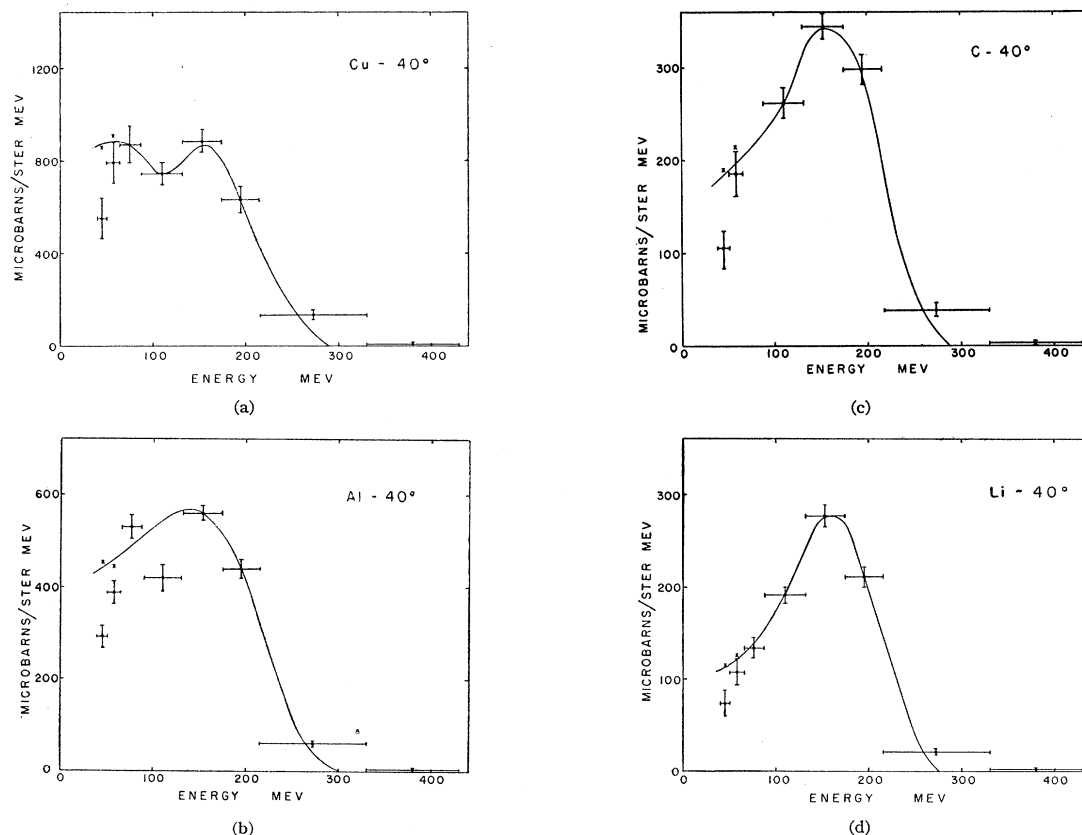
FIG. 10. Proton differential cross sections.

pointed out that the 0° deuteron spectrum from carbon found by Hadley and York looked similar to the incident 87-Mev neutron spectrum displaced to a 65-Mev peak; this gives $B=13$ Mev.

Curves constructed in the method outlined above, using $n=1, 2, 3, 4,$ and $6,$ are shown in Fig. 15 with the corresponding experimental deuteron spectra superimposed on them. The areas under these curves above 50 Mev have been measured and are listed in Table III. The last column in the table lists the values for the pick-up probability found when the sum of the experimentally measured differential cross sections for deuteron production at the three angles used were made to agree with the sum of the same cross sections as calculated by the method of this section.

It appears that the energy dependence of the pick-up probability is best given by E^{-2} or E^{-3} .

There have been other estimates of this energy dependence of the pick-up process. Heidmann,⁷ using the Born approximation, obtained a value of $n=6$. Bratenahl,⁸ using deuterium for the target nucleus, has obtained a value of $n=3$ experimentally. Slater,⁹ at this laboratory, in studying (d,p) reactions which are the inverse of the pick-up process, found an energy dependence which for energies higher than 50 Mev is given by $n=2$ for several heavy elements. In the analysis by Chew and Goldberger,³ the cross section obtained has roughly an E^{-2} energy dependence.

FIG. 11. Energy spectra of protons at 40° to the beam for various elements bombarded with 300-Mev protons.

⁷ J. Heidmann, Phys. Rev. **80**, 171 (1950).

⁸ A. Bratenahl (private communication).

⁹ L. M. Slater, University of California Radiation Laboratory Report No. UCRL-2441, March, 1954 (unpublished).

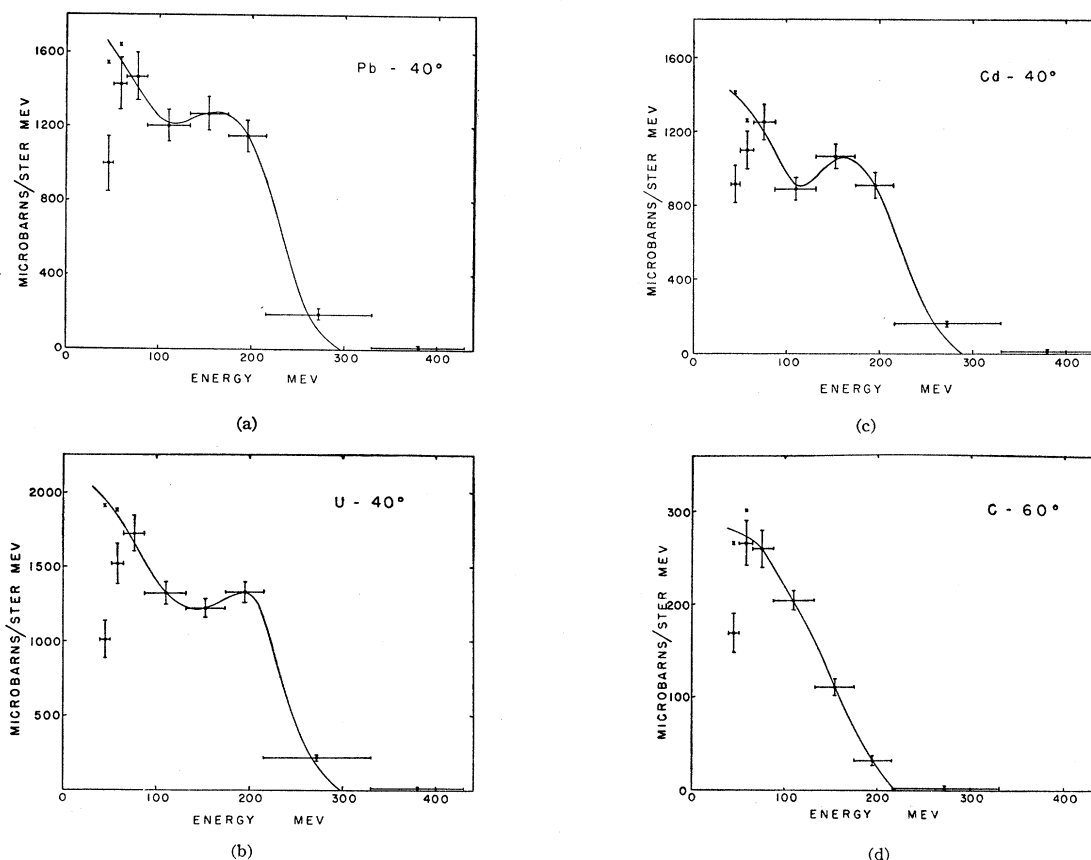


FIG. 12. Energy spectra of protons at 40° or 60° to the beam for various elements bombarded with 300-Mev protons.

V. RESULTS AND CONCLUSIONS

A. Proton Yields and Energy Spectra

The differential cross section for scattering protons from light elements here observed at 40° to the 300-Mev proton beam can be written as

$$\sigma_{(p+X \rightarrow p)}(40^\circ) = kA^{0.72}.$$

Dr. Warren Heckrotte predicted an exponent of 0.78 on the basis of the theory of a semitransparent nucleus.¹⁰ A recent measurement of proton nuclear absorption cross sections¹¹ gave an exponent for *A*-dependence of 0.73 for high-energy incident protons.

Proton-energy spectra are shown for various elements at various angles in Figs. 11, 12, and 13. The spectrum from carbon at 40° compares well with Cladis's curve⁵ for the same spectrum. The quasi-elastic peak stays visible all the way to uranium, but the background of multiple-nucleon collision events of course becomes larger with increasing values of *A*.

¹⁰ Fernbach, Serber, and Taylor, Phys. Rev. **75**, 1352 (1949).

¹¹ A. J. Kirschbaum, University of California Radiation Laboratory Report No. UCRL-1967, October, 1952 (unpublished); and Phys. Rev. **90**, 449 (1953).

B. Dependence of Deuteron Production Cross Sections on *A*

According to the data of this experiment the differential cross section for deuteron production from light elements (lithium, carbon, and aluminum) at 40° to an incident proton can be written as

$$\sigma_{(p+C \rightarrow d)}(40^\circ) = kA^{1.2}.$$

This strongly suggests that the mechanism that produces these deuterons is the indirect pickup process described above. It has been shown in the preceding paragraph that the differential cross section for quasi-

TABLE III. Areas under the curves of Fig. 15.^a

Angle to beam	26°	40°	60°	Expression used for pickup probability	
Measured value	1.78 ± 0.41	1.90 ± 0.35	1.42 ± 0.30	...	
Calculated by using	E^{-1}	2.39	1.61	1.19	0.093(<i>E</i> /100) ⁻¹
	E^{-2}	1.88	1.68	1.63	0.115(<i>E</i> /100) ⁻²
	E^{-3}	1.69	1.70	1.80	0.138(<i>E</i> /100) ⁻³
	E^{-4}	1.53	1.72	1.94	0.138(<i>E</i> /100) ⁻⁴
	E^{-6}	1.26	1.70	2.23	0.122(<i>E</i> /100) ⁻⁶

^a All cross sections given in millibarns/steradian. All energies given in Mev.

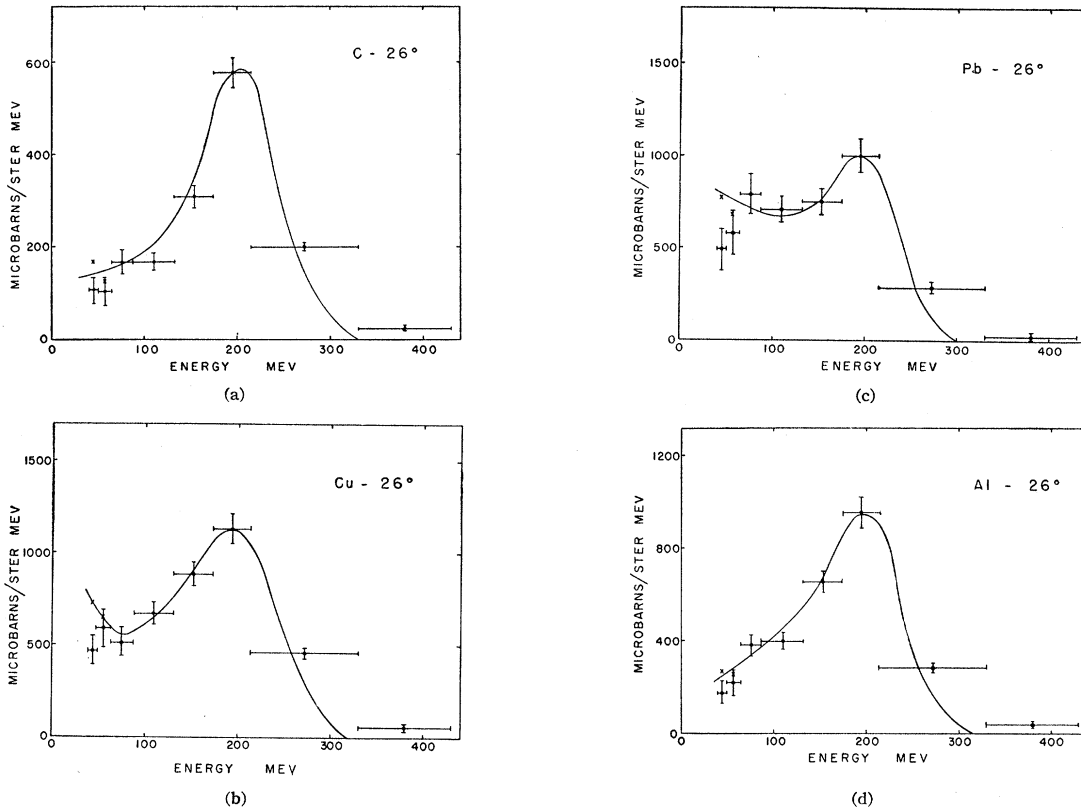


FIG. 13. Energy spectra of protons at 26° to the beam for various elements bombarded with 300-Mev protons.

elastic nucleon scattering goes as $A^{0.72}$. Also, the A dependence of the direct pickup process is known from the work of Hadley and York.² The total cross sections measured by Hadley and York for making direct pickup deuterons from carbon and copper indicate an exponent of 0.41. Now, returning to the direct pick-up deuterons, we have

$$\begin{aligned} \sigma_{\text{indirect pickup}} &= [\sigma_{\text{nucleon scattering}}][\text{Pick-up probability}] \\ &= [C_1 A^{0.72}][C_2 A^{0.41}] = C_1 C_2 A^{1.13}. \end{aligned}$$

The exponent here is close to that mentioned in the foregoing. It should be noted that the A -dependence of the pick-up part of this process implies that the pickup occurs on the surface of the nucleus. That is, the exponent 0.41 shows that as the target nucleus becomes larger only part of the added nucleons are important in producing the pick-up deuterons. Since the mean free path of deuterons in nuclear matter is small compared to nuclear dimensions, the important nucleons are ex-

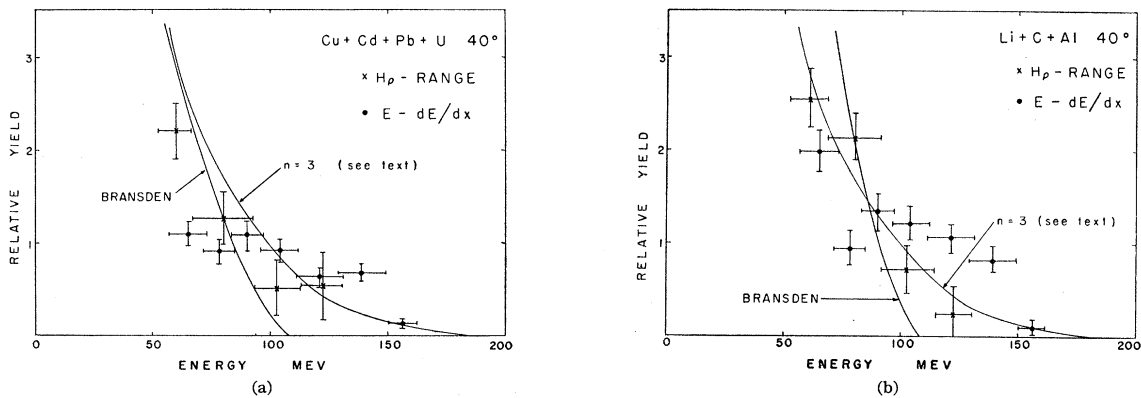


FIG. 14. Energy spectra of deuterons at 40° to the beam for light and heavy elements bombarded with 300-Mev protons.

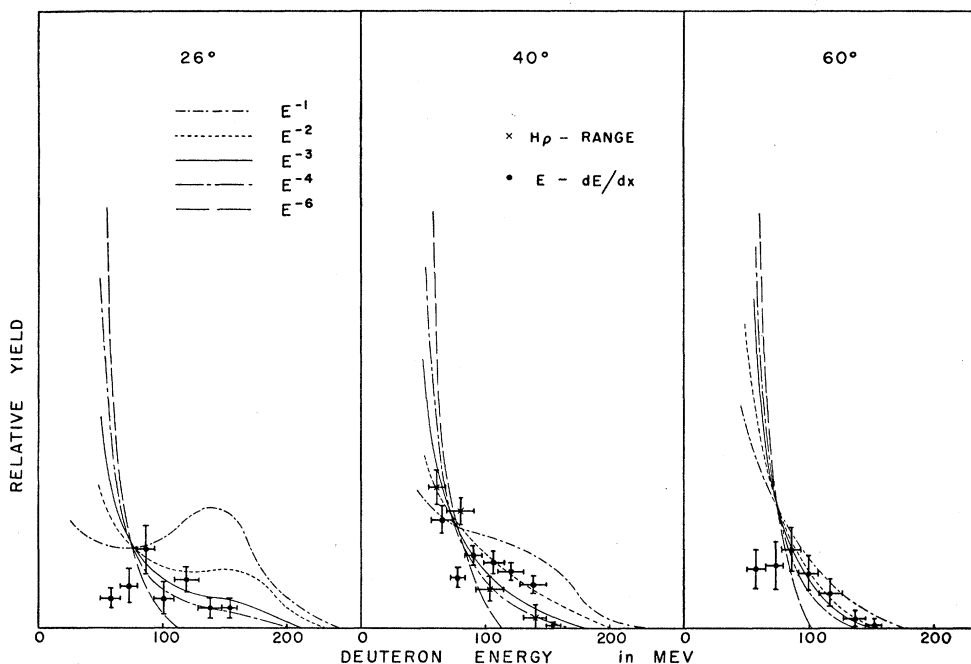


FIG. 15. Deuteron energy spectra calculated by using the indirect pick-up process and assuming the energy dependence of the pick-up process to be given by E^{-n} . Values of n of 1, 2, 3, 4, and 6 were used in the calculation.

pected to be the surface nucleons; but apparently not all of these are effective, in view of the value of 0.41 instead of approximately $\frac{2}{3}$.

Above copper the heavier elements in this experiment do not obey the same A dependence as the light elements in the production of deuterons. The value of the exponent here is about 0.6. Stuart¹² has shown that electric-field stripping of the emergent deuterons should not be responsible for this heavy-element A -dependence. The effect that provides the most reasonable explanation has to do with the pick-up probability. Since the pickup takes place on the surface of the nucleus, the area of the surface that can be effective in the pick-up process is limited by the fact that a deuteron cannot be formed if the two nucleons involved are farther apart than they can be in a deuteron.

The radius of the copper nucleus is larger than the nominal size of the deuteron ($\sim 4 \times 10^{-13}$ cm). Therefore, it is not surprising that for nuclei larger than copper the additional surface area is not effective in producing deuterons, and that as a result the pick-up part of an indirect pick-up process for heavy elements is independent of A . Selove¹³ has found that the direct pick-up differential cross sections at 18° for making deuterons from copper and lead are essentially equal, also indicating that $n=0$ for this case. As a result of this, all the A -dependence of the indirect pick-up process for heavy elements is given by the nucleon-scattering A dependence, which for heavy nuclei is about $n=0.5$ (see Fig. 10).

¹² R. N. Stuart, University of California Radiation Laboratory Report No. UCRL-2574 (unpublished).

¹³ W. Selove, Phys. Rev. **92**, 1328 (1953); and private communication.

C. Deuteron Angular Distribution and Energy Spectra

The angular distribution of deuterons from proton bombardment of carbon is shown in Fig. 16. On the figure are the theoretical curve of Bransden¹⁴ and the curve obtained by the method of Sec. IV of this report by using $n=2$. The experimental distribution is seen to be quite flat over the angular interval measured. The Born approximation curve of Bransden is normalized to a total cross section in carbon of 9 millibarns. It appears to be too much peaked forward. The height of the curve calculated by the method of Sec. IV has been adjusted to the experimental data by arbitrarily choosing the value of k in $P = kE^{-n}$. (See Table III.)

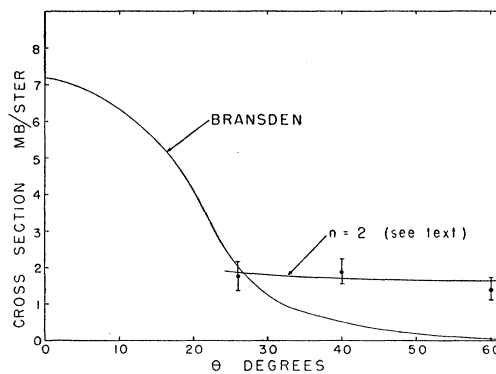


FIG. 16. Angular distribution of deuterons.

¹⁴ The author is deeply indebted to Dr. B. H. Bransden and Mr. J. McKee of Queens University, Belfast, Ireland, for extending the calculations of reference 3 to obtain the energy spectra and angular distribution of deuterons shown in Figs. 14 and 16.

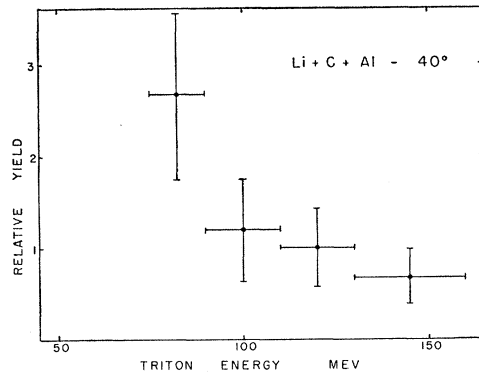


FIG. 17. Energy spectrum of tritons at 40° to the beam for light elements bombarded with 300-Mev protons.

The deuteron energy spectra at 40° are shown in Fig. 14. The energy spectra calculated by Bransden and by the method of Sec. IV are shown on these figures. The Bransden spectra seem to have somewhat too low an energy cutoff. It is noted that the 45° deuteron energy spectrum by Hadley and York resembles the indirect deuteron spectra obtained in this experiment.

During an analysis of 300-Mev neutron-induced stars in oxygen, Fuller¹⁵ has recently found a considerable yield of high-energy deuterons (>20 Mev) having an energy spectrum and angular distribution very similar to the deuterons observed in this experiment.

D. Tritons

As shown in the mass spectrum in Fig. 8, there is a measurable yield of tritons observed at wide angles to a 300-Mev nucleon beam. Cross sections for triton production are given in Tables I and II. If we work out a least-squares fit to the data for Li, C, and Al, we get

$$\sigma_{(p+\alpha \rightarrow t)}(40^\circ) = kA^{1.28}.$$

This A -dependence is very similar to the deuteron A dependence, which would imply that the tritons also are formed by the indirect pick-up process. The energy spectrum for tritons from proton bombardment of light elements at 40° to the beam is shown in Fig. 17, and is similar to the deuteron spectra, as might be expected if the same mechanism of formation is involved.

VI. SURFACE NUCLEONS

It has been demonstrated that the indirect pickup deuterons are made near the nuclear surface. Because of this fact we can get some information about the variety of nucleons found on the surface of the nucleus if we perform two experiments, using first an incident proton beam and then an incident neutron beam.

First, let us consider the indirect pickup deuterons resulting from proton bombardment. Figure 18(A)

shows this event. For nuclei with nearly equal numbers of neutrons and protons a simple cross section argument would lead one to expect about three times as many scattered protons as neutrons in the scattered-nucleon beam. As most of the scattered nucleons are protons, then the particles that are picked up at the nuclear surface to form deuterons are mostly neutrons.

In the performance of an incident-neutron beam experiment as shown in Fig. 18(B), the same argument leads one to expect more scattered neutrons than protons in a ratio of approximately 3:1. With a neutron beam incident the scattered nucleons, consisting mainly of neutrons, must pick up protons at the nuclear surface to form deuterons. In this way the yield of deuterons from a proton beam experiment depends strongly upon the presence of neutrons on the nuclear surface, and the deuterons from a neutron beam experiment depend upon the presence of protons on the nuclear surface.

Using the method outlined in Sec. VII, we obtain values for the fraction x of "surface" nucleons that are neutrons. The values of x are shown on Fig. 19. The crosses are the volume fraction of nucleons that are neutrons. This is given by

$$\text{Number of neutrons/atomic number} = N/A.$$

The experimental values of x for light elements (lithium and carbon) lie on the curve of N/A , indicating that for light elements the surface nucleons are not to be distinguished from the nucleons in the rest of the nucleus. For heavier elements, especially lead and uranium, the experimental value of x lies significantly above the N/A curve. The average of the x values for the four heaviest elements lies almost three standard deviations above the N/A line. This indicates that there may be an excess of neutrons on the nuclear surface, if the foregoing interpretations are correct.

Actually, the "surface" as defined by this experiment has some depth, being the region in which the pickup part of the indirect pick-up process takes place. An estimate of the depth of this "surface" based on Bransden's calculations gives 1.8×10^{-13} cm.

If we use a simple model and assume that there is a nuclear skin composed of neutrons only, we can get an

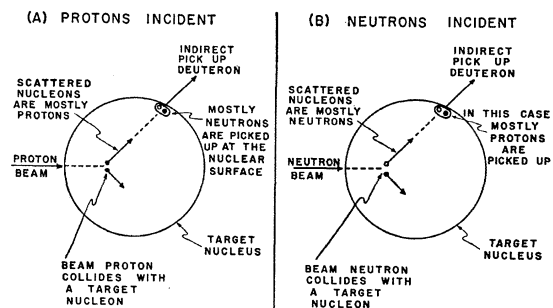


FIG. 18. Schematic diagram of the indirect pickup process using (A) a proton beam or (B) a neutron beam incident on the target.

¹⁵ M. O. Fuller, University of California Radiation Laboratory Report No. UCRL-2699, September, 1954 (unpublished).

estimate of its thickness,

$$lx = s + (l-s)(N/A),$$

where l = depth of surface layer within which pickup occurs = 1.8×10^{-13} cm (from Bransden), x = average fraction of nucleons in this region that are neutrons = 0.78 (from this experiment for Pb), and s = thickness of assumed "skin" of neutrons. For Pb, for which $N/A = 0.60$, the value of s thus obtained is 0.8×10^{-13} cm.

Measurements of nuclear radii by methods that involve the charge distribution¹⁶ and by methods that involve the nuclear potential distribution¹⁷ tend to substantiate this viewpoint. The charge-distribution radii appear to be smaller than those determined by high-energy neutron collisions, thus suggesting the presence of surface neutrons. The best value of the coefficient for the square-well-radius as obtained from the charge distribution experiments is about $r_0 = 1.20 \times 10^{-13}$ cm, and for the nucleon distribution the value is about $r_0 = 1.37 \times 10^{-13}$ cm. The charge-distribution radius is smaller, but part of the difference may be due to the range of nuclear forces. Neglecting the effect of the range of nuclear forces, we can estimate a value for the neutron skin thickness from these data. Considering lead,

$$s \approx \Delta r_0 A^{1/3} = (207)^{1/3} (1.37 - 1.20) \times 10^{-13} = 1.0 \times 10^{-13} \text{ cm.}$$

The neutron skin effect has also been postulated theoretically¹⁸ as being a result of the Coulomb potential. The value of s in that analysis is thought to be about $\frac{1}{2}$ the meson Compton wavelength, $s \approx \frac{1}{2} (\hbar/\mu c) = 0.7 \times 10^{-13}$ cm.

It has been suggested that a difference in the momentum distributions of surface neutrons and protons could be responsible for the difference in the indirect pickup deuteron yields upon proton or neutron bombardment, interpreted here as being due to a difference in surface populations of protons and neutrons. If the neutrons on the surface have a higher average momentum, then according to the analysis of Chew and Goldberger there is a larger probability that neutrons will be picked up than protons. A reason why neutrons may have larger momenta is that the potential well is deeper for neutrons than for protons, owing to the Coulomb potential. But the fact that the proton wave function is depressed more steeply than the neutron wave function, because of the Coulomb barrier, implies that the proton wave function has more curvature near the edge of the well, therefore contributing to high-momentum components for the protons. It is not ob-

¹⁶ Lyman, Hanson, and Scott, Phys. Rev. **84**, 626 (1951); V. L. Fitch and J. Rainwater, Phys. Rev. **92**, 789 (1953); F. Bitter and H. Feshbach, Phys. Rev. **92**, 837 (1953).

¹⁷ Cook, McMillan, Peterson, and Sewell, Phys. Rev. **75**, 7 (1949); Bratenahl, Fernbach, Hildebrand, Leith, and Moyer, Phys. Rev. **77**, 597 (1950); Warren Heckrotte, University of California Radiation Laboratory Report No. UCRL-2510, March 1954 (unpublished).

¹⁸ M. H. Johnson and E. Teller, Phys. Rev. **93**, 357 (1954).

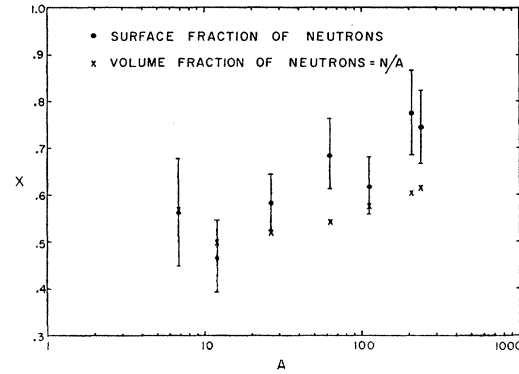


FIG. 19. The fraction of surface nucleons that are neutrons for various elements.

vious whether the net effect is to make the average surface neutron momentum larger or smaller than the surface proton momentum.

Swiatecki,¹⁹ considering why the nuclear surface energy is as large as it is, has developed a nuclear model that bears on this problem. This new model has sloping sides in which the rise occurs in a distance of 6 to 8×10^{-13} cm. In a Fermi gas, if there are more neutrons than protons in the nucleus, then the zero-point energies for neutrons are larger than for protons. These faster neutrons explore greater volumes of space and therefore result in a larger effective radius for neutrons. This model then gives faster neutrons, and also neutrons existing at larger radii than protons. Both these effects could contribute to the observed deuteron yields.

VII. DETERMINATION OF THE FRACTION OF SURFACE NUCLEONS THAT ARE NEUTRONS

As in Sec. IV, we can write, for the cross section for deuteron production from protons bombarding element A , a product of a nucleon-scattering cross section and a pick-up probability:

$$\sigma_{(p+A \rightarrow d)}(\theta) = \sigma_{(p+A \rightarrow p)}(\theta)P_1 + \sigma_{(p+A \rightarrow n)}(\theta)P_2.$$

Similarly, for neutrons bombarding element A , we can write

$$\sigma_{(n+A \rightarrow d)}(\theta) = \sigma_{(n+A \rightarrow p)}(\theta)P_1 + \sigma_{(n+A \rightarrow n)}(\theta)P_2.$$

Now if we separate the scattering in nucleus A into scattering from protons and neutrons we can write

$$\sigma_{(p+A \rightarrow p)}(\theta) = (Z)\sigma_{(p+p \rightarrow p)}(\theta) + (A-Z)\sigma_{(p+n \rightarrow p)}(\theta),$$

$$\sigma_{(n+A \rightarrow p)}(\theta) = (Z)\sigma_{(n+p \rightarrow p)}(\theta),$$

$$\sigma_{(p+A \rightarrow n)}(\theta) = (A-Z)\sigma_{(p+n \rightarrow n)}(\theta),$$

$$\sigma_{(n+A \rightarrow n)}(\theta) = (A-Z)\sigma_{(n+n \rightarrow n)}(\theta) + (Z)\sigma_{(n+p \rightarrow n)}(\theta).$$

The cross sections on the right above are nucleon-nucleon cross sections averaged over a range of energies attributable to the internal momentum of the struck nucleon, and otherwise modified so as to be appropriate to collisions within the nucleon well. They do not need

¹⁹ W. J. Swiatecki, Phys. Rev. **98**, 203 (1955).

TABLE IV. Fraction x of nucleons in the pick-up region that are neutrons.

Element	x from single scattering	x from double scattering
Li	0.564	0.652
C	0.470	0.458
Al	0.585	0.609
Cu	0.684	0.732
Cd	0.620	0.708
Pb	0.775	0.859
U	0.745	0.845

to be explicitly evaluated, as is evident in the following discussion.

In the course of the experiment we measure four cross sections.

$$\begin{aligned} \sigma_{(p+A \rightarrow d)}(\theta), \quad \sigma_{(p+A \rightarrow p)}(\theta), \\ \sigma_{(n+A \rightarrow d)}(\theta), \quad \sigma_{(n+A \rightarrow p)}(\theta). \end{aligned}$$

Using these data and above equations, we must make two simplifying assumptions in order to proceed:

$$\begin{aligned} \sigma_{(n+n \rightarrow n)}(\theta) &= \sigma_{(p+p \rightarrow p)}(\theta), \\ \sigma_{(p+n \rightarrow p)}(\theta) &= \sigma_{(n+p \rightarrow p)}(\theta) = \sigma_{(p+n \rightarrow n)}(\theta) = \sigma_{(n+p \rightarrow n)}(\theta). \end{aligned}$$

The first assumption says that $n-n$ scattering is the same as $p-p$ scattering, for which there is considerable evidence. The second says that the $n-p$ differential cross section in the center-of-mass system is symmetrical about 90° . This is very nearly true in the case of free $n-p$ collisions²⁰ for angles from 40° cm to 140° cm, which covers the angular interval of interest. The fact that these events take place in the nucleus rather than as isolated events is assumed to not change the picture appreciably. For simplicity we call the cross sections on the left-hand side in the above equations σ_{pp} and σ_{np} . These should not be taken to be free nucleon-nucleon cross sections. Substituting, we get

$$\begin{aligned} \sigma_{(p+A \rightarrow d)}(\theta) &= Z\sigma_{pp}P_1 + (A-Z)\sigma_{np}P_1 + (A-Z)\sigma_{np}P_2, \\ \sigma_{(n+A \rightarrow d)}(\theta) &= Z\sigma_{np}P_1 + (A-Z)\sigma_{pp}P_2 + Z\sigma_{np}P_2. \end{aligned}$$

Now let us consider the pick-up probabilities. We have $P = kN$, where N = number of available partner nucleons. The proportionality constant k is the same for a proton picking up a neutron as for a neutron picking

up a proton:

$$\begin{aligned} P_1 &= kN_1, \quad N_1 = lax, \\ P_2 &= kN_2, \quad N_2 = la(1-x), \end{aligned}$$

where N_1 = number of available neutrons, N_2 = number of available protons, a = effective surface area within which pickup event occurs (related to size of deuteron), l = effective depth of pick-up region, and x = fraction of nucleons in the pick-up region that are neutrons. Substituting in preceding equation and taking a ratio, we obtain

$$R = \frac{\sigma_{(n+A \rightarrow d)}(\theta)}{\sigma_{(p+A \rightarrow d)}(\theta)} = \frac{Z\sigma_{np}x + [(A-Z)\sigma_{pp} + Z\sigma_{np}](1-x)}{[Z\sigma_{pp} + (A-Z)\sigma_{np}]x + (A-Z)\sigma_{np}(1-x)}.$$

Taking the ratio of the measured proton-production cross sections,

$$Q = \frac{\sigma_{(p+A \rightarrow p)}(\theta)}{\sigma_{(n+A \rightarrow p)}(\theta)} = \frac{Z\sigma_{pp} + (A-Z)\sigma_{np}}{Z\sigma_{np}} = \frac{\sigma_{pp}}{\sigma_{np}} + \frac{A-Z}{Z},$$

and substituting this into the previous equation and solving for x , we have

$$x = \left[\left(\frac{Z}{A-Z} \right) + Q - \left(\frac{A-Z}{Z} \right) - R \right] / \left\{ \left[R \left(\frac{Z}{A-Z} \right) + 1 \right] \left(Q - \frac{A-Z}{Z} \right) \right\}.$$

The values of x can be obtained from this equation by using the experimental data.

If a similar analysis is carried out for only those events in which the incident nucleon is scattered twice before it picks up to form a deuteron, the results are not much different from the single-scattering analysis. The values of x are slightly larger, especially for heavy nuclei (see Table IV).

The nucleons that pick up to form deuterons result from a combination of single-scattering events, double-scattering events, and more complicated events. The double-scattering events become more important for heavy nuclei. Because of this, the surface neutron surplus in heavy elements is, if anything, larger than that indicated in Fig. 19, owing to complex scattering events.

²⁰ Chung Ying Chih, University of California Radiation Laboratory Report No. UCRL-2575, May, 1954 (unpublished); J. DePangher, University of California Radiation Report No. UCRL-2153, March, 1953 (unpublished).